Journal of Sustainable Metallurgy (2019) 5:127–140
https://doi.org/10.1007/s40831-018-0201-5

REVIEW ARTICLE

A Review on Reclamation and Reutilization of Ironmaking and Steelmaking Slags

Zhanjun Wang[1] · Il Sohn[1]

Published online: 12 December 2018

Abstract
Ironmaking and steelmaking slags are the dominant byproducts in metallurgical processes, and the up-cycling and recycling of slags are essential to the sustainability of the metallurgical industry. As the metallurgical slags contain significant valuable elements, these slags can be re-utilized as a stand-alone product or as additives for other products after valuable elements are effectively separated. Several areas for slag application are discussed in this review including internal reuse of the slag within the metallurgical process, civil construction and building materials, and future potential applications. To ensure greater reclamation of the slags, fundamental studies regarding crystallization and elemental redistribution of the metal cation in the slags are also examined.

Keywords Ironmaking slags · Steelmaking slags · Reclamation · Crystallization · Elemental re-distribution

Introduction

Over recent decades, the crude steel production in the whole world has significantly grown and reached an estimated 1700 million tons in 2017, with China accounting for about half the world's crude steel production, as shown in Fig. 1a, b [1, 2]. This vast amount of global steel production inevitably generates significant amounts of byproducts during processing, which include approximately 500 million tons of slags, as shown in Fig. 1c [1, 3]. Due to the large amounts of slag produced from the use of low-grade iron ore, it is essential to efficiently utilize these byproducts as secondary resources to increase steel sustainability [4, 5]. In particular, metallurgical slags from the ironmaking and steelmaking operations require immediate attention to minimize excessive landfilling and environmental pollution and increase the effective land mass for farming. The recovery rate of slags in developed countries has reached nearly 100 pct for ironmaking slags and up to 80 pct for steelmaking slags, but the steelmaking slags are often used in lower value-added products such as road-bed construction. Compared with the developed countries, the recovery rates of slags in China lag behind—with the recovery rates of ironmaking and steelmaking slags in China being only 70–80 pct and 20–30 pct, respectively [1, 2].

The relatively lower recovery rate for ironmaking slags in China compared to the developed countries can be ascribed to the use of more complex minerals, especially the titaniferous magnetite ores, and greater number of small- and medium-sized enterprises with limited infrastructures and capital to treat the slags. In addition, due to the increased use of low-grade iron ore, the steelmaking slags can inevitably contain large amounts of phosphorus and sulfur impurities, which will cast a burden on downstream treatment and further limit the recycling proportion of steelmaking slags. The presence of free-CaO and MgO, Fe_tO, MnO, P_2O_5, and other heavy metals in the steelmaking slags has also been speculated to be a hurdle in the utilization of steelmaking slags [6–8]. In terms of the environmental and economic benefits of slag recycling, there iare significant un-utilized or disposed portions of the slags that have the potential to be more effectively utilized. Some of these metallurgical slags can be treated and used as secondary resources for other industries depending on its overall contents of valuable elements. Works on selective crystallization and phase separation of valuable elements in

The contributing editor for this article was Sharif Jahanshahi.

✉ Il Sohn
ilsohn@yonsei.ac.kr

[1] Department of Materials Science and Engineering, Yonsei University, Seoul 120-749, Korea

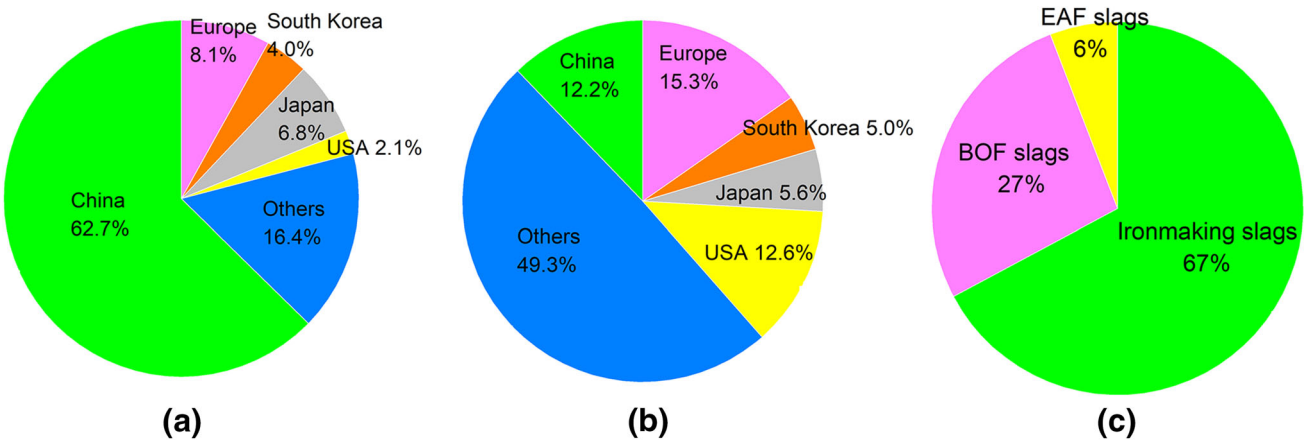

Fig. 1 **a** Global steel production proportion from integrated steel (about 1210 million tons in 2017) by country. **b** Global steel production proportion from EAF steel (about 420 million tons in 2017) by country. **c** Global estimated slag production (about 500 million tons in 2017) proportion according to processing route (Color figure online). Adapted from Worldsteel Association [1], Guo et al. [2], and Nippon Slag Association [3]

metallurgical slags have been carried out to consider the reuse of the valuable elements [9–12], where specific elemental enrichment in phases such as $nCa_2SiO_4{\cdot}Ca_3P_2O_8$ can be selectively grown and separated to be used as a phosphorus resource.

Since molten slags of iron and steel generally have high temperatures greater than 1773 K (1500 °C), these slags can be naturally or forced cooled. With natural cooling, the valuable elements are relatively dispersed and highly crystallized with a low utilization capacity. With controlled cooling, the crystallization phase of the slags can be adjusted by means of different additives or through controlling the cooling rate to precipitate a target phase that is in line with the efficient utilization of slags. Zhao et al. [13] investigated slag wool fabrication using high-temperature blast furnace (BF) slags modified by coal ash, where a slag viscosity between 0.5 and 2.5 Pa s and a superheat temperature of 50 °C above the liquidus temperature were necessary to guarantee good fluidity and avoid crystallization. The proportion of amorphous phase in BF slags treated by different cooling systems is also an important indicator affecting the activity and strength of slag cement, where a comparable performance to the ordinary Portland cement can be achieved when the amorphous phase proportion exceeded 90 pct [14]. Hence, the physicochemical properties of high-temperature molten slags are fundamental to developing suitable methods to efficiently use valuable materials in metallurgical slags.

This review aims to provide fundamental works on slag recycling and application to the ironmaking and steelmaking slags and the potentials of future use for enhanced sustainability of the industry.

Characteristics of Ironmaking and Steelmaking Slags

The chemical compositions of different types of metallurgical slags are schematically illustrated in Fig. 2 [15]. The water-quenched ordinary Ti-free BF slags are amorphous, which can be used as raw materials for cement production. However, Ti-bearing BF slags with high TiO_2 content have a strong crystallization ability, which leads to relatively low proportion of amorphous phase during cooling and a low cementitious property, which limits the allowable amount of Ti-bearing BF slags for utilization as a cement additive. As for steelmaking slags, the chemical composition can vary according to the furnace type, steel grades, and pretreatment method [16]. The main mineral phases contained in steelmaking slags are dicalcium silicate (Ca_2SiO_4), tricalcium silicate (Ca_3SiO_5), RO phase (CaO–FeO–MnO–MgO solid solution), tetra-calcium aluminoferrite (Ca_4AlFeO_7), merwinite, and free-CaO. In addition, toxic elements (e.g., Cd, Cr, and As) are also present in some metallurgical slags, which make it hazardous and unacceptable for landfill [17].

The physicochemical properties of the slags are crucial in treating the slags, including viscosity, surface tension, electrical conductivity, etc. According to the structural properties, the slags compositions can be divided into network modifiers (e.g., CaO, MgO, Na_2O, K_2O, FeO, etc.), network formers (e.g., SiO_2, P_2O_5), and amphoteric oxides with the above two behaviors (e.g., Al_2O_3). The structure behavior of the chemical compositions causes an essential effect on the viscosity of the molten slags and further determines the mass-transfer behavior during the crystallization, where an increase in NBO/T (non-bridging

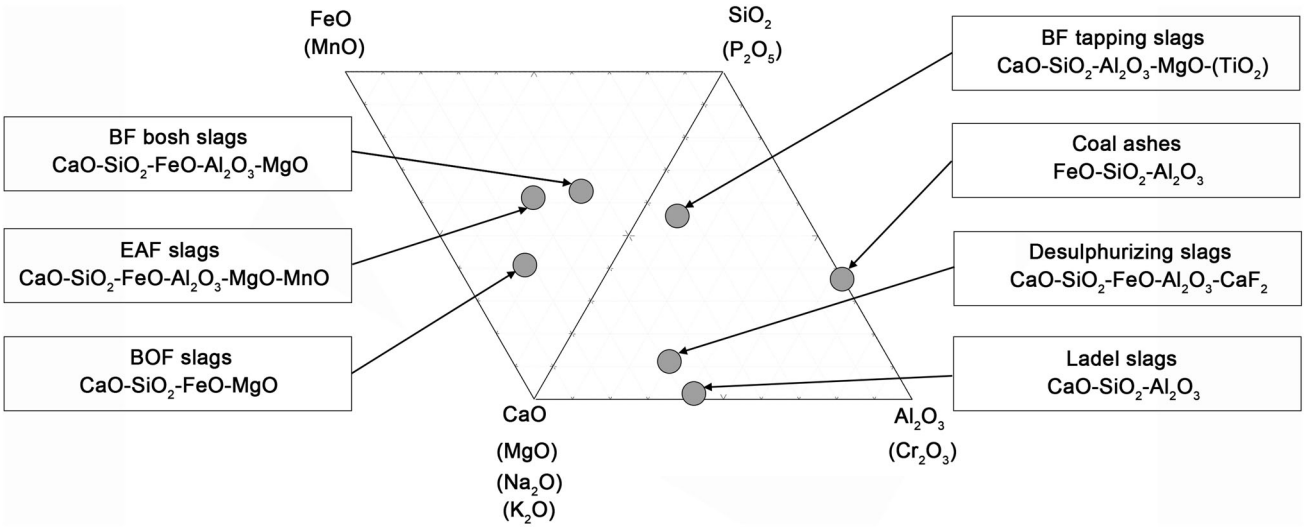

Fig. 2 Schematic illustration of the chemical compositions for different types of metallurgical slags within the pseudoternary phase diagram. Adapted from Min and Tsukihashi [15]

oxygen per network former) corresponds to structural depolymerization, decreasing viscosity, and acceleration of mass transfer. Surface tension of the molten metallurgical slags is also an important parameter affecting various interfacial phenomenon during ironmaking and steelmaking process such as slag-metal, metal-refractory, and slag-refractory interfaces. The surface tension increases with the increasing ionization potential for network-modifiers, while it shows an opposite trend for the network formers. It can be inferred that the increase in surface tension is due to the interaction between network modifiers and oxygens increasing the strength of the surface bonds, while network formers and oxygens generate a covalent with the overwhelming bond strength to reduce the surface tension. In addition, the electrical conductivity of the EAF slag for remelting is directly related to the electricity system and heat distribution, which is also associated with slag structure that it increases with depolymerization of the slags [15].

Fundamentals for Greater Recycling of Ironmaking and Steelmaking Slags

Recovery of Valuable Elements from Ironmaking Slags

Depending on the raw materials availability and the expanded use of low-grade sources of iron oxides, titaniferous magnetite ores have been utilized. The use of these ores can result in higher concentrations of TiO_2 in BF slags, which can be recycled as a secondary source for TiO_2. For typical BF operations that utilize higher-grade hematite-based ores of goethite and martite, the Ti-free BF slags can often find uses for cement applications [18, 19]. The strong crystallinity of Ti-bearing BF slags leads to a narrow range of its applications, such as the preparation of photocatalytic materials [20, 21] and the preparation of titanium alloys [22], while its complex process and high cost limit its usage amount. Based on the typical compositions of the BF slags in some factories, utilizing Ti-bearing BF slags as a secondary source for TiO_2 can be possible, if the enrichment and separation can be improved. However, optimizing the enrichment and separation of TiO_2-enriched phases requires a fundamental understanding of the crystallization phenomena.

Li et al. [23–26] and Hu and co-workers [27–32] investigated the crystallization behavior of synthesized Ti-bearing BF slags using single hot thermocouple technique (SHTT) and confocal laser scanning microscopy (CLSM), respectively. Depending on the incorporation of TiO_2 into different crystal phases, the separation efficiency and concentration of TiO_2 for secondary resources could be ascertained. Figure 3a, b shows the SHTT result of the Ti-enriched phase transformed from rutile (TiO_2) with a rod-shaped crystal to perovskite ($CaTiO_3$) with a dendritic-shaped crystal when the basicity (mass ratio of CaO to SiO_2) increased from 0.6 to 1.0. Figure 3c shows a similar dendritic-shaped perovskite crystal observed from the CLSM with a high resolution. During the crystallization experiments, it was found that the Ti-enriched and depleted phases have significantly different precipitation temperatures, where the Ti-enriched phase can be initially formed within a wide isothermal temperature range spanning 160 °C, and $CaMgSi_2O_6$, $CaAl_2Si_2O_8$, and $CaTiSiO_5$ were precipitated at lower isothermal temperatures. The large

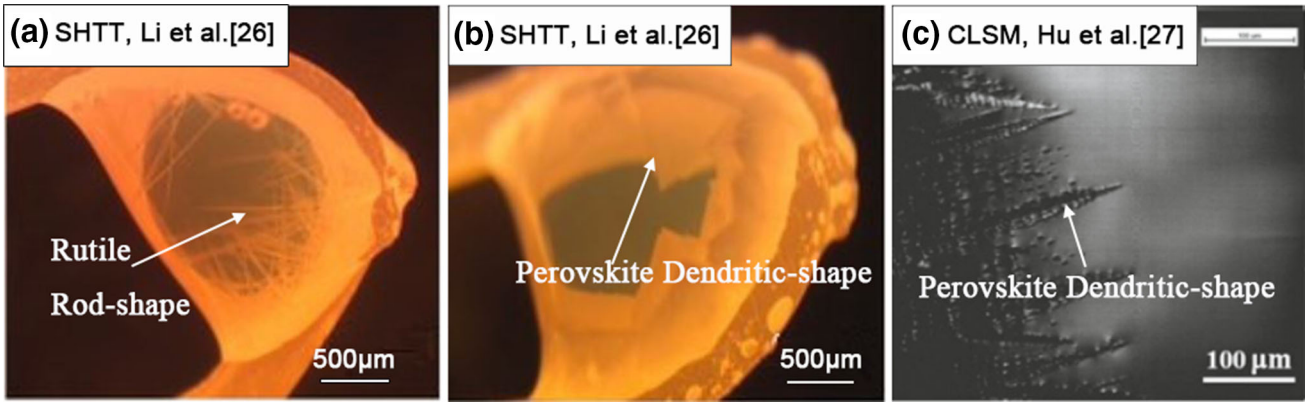

Fig. 3 **a** SHTT images with C/S = 0.6 and TiO_2 = 25 wt pct, **b** SHTT images with C/S = 1.0 and TiO_2 = 25 wt pct, and **c** CLSM images with C/S = 1 and TiO_2 = 20 wt pct (Color figure online). Adapted from Li et al. [26] and Hu et al. [27]

difference in the crystallization temperatures facilitates the separation of different phases with different concentrations of Ti. To stimulate the crystallization behavior and enhance the differences between phases, the effect of oxygen partial pressure on the formation of Ti-enriched phase under a C/CO equilibrium atmosphere was studied [25]. It was shown that the primary perovskite ($CaTiO_3$) crystal phase transformed to an anosovite (Ti_2O_3) phase under reducing conditions, while it transformed to rutile (TiO_2) crystal phase under oxidizing conditions. Considering that TiO_2 is generally lower than 25 wt pct in BF slags, perovskite was mainly considered as the Ti-enriched phase. At higher basicities, TiO_2 and CaO preferentially diffuse to the surface forming perovskite and replacing other Ti-containing phases formed at lower basicities. Zhang et al. [33, 34] indicated lower cooling rates favored the nucleation and growth of rutile in Ti-bearing BF slags, and Wang et al. [35] constructed the crystallization curves of Ti-enriched phases within a broad range of compositions. Based on the above work, the crystallization behavior of Ti-enriched phase could also be enhanced with the additions of Al_2O_3 [36], B_2O_3 [37], and ZrO_2 [38]. Higher Al_2O_3 content can promote a change of the primary crystal phase to $Mg_3Al_4Ti_8O_{25}$, followed by a higher crystallization temperature and a lower incubation time, suggesting an acceleration of crystallization. Li et al. [38] also observed greater incubation times of the primary rutile phase with additions of ZrO_2 from 0 to 3 wt pct, which were subsequently shortened by raising ZrO_2 additions up to 5 wt pct. This may be explained by the competitive effects of the inhibited nucleation of the crystals due to the increased viscosity and the accelerated nucleation of the crystals through the larger driving force caused by the higher undercooling with the increasing ZrO_2 content. Sun et al. [37] described the results of adding small amounts of B_2O_3 to inhibit the precipitation of perovskite and effectively promote the transformation of the primary phase from perovskite to rutile. The lowering of the incubation time with higher B_2O_3 can be ascribed to the enhancement of the crystallization with a lower viscosity [39].

For Ti-free BF slags, the slags can be used as raw materials for cement. The dominant precipitated phases in continuously cooled BF slags have been found to be akermanite ($2CaO{\cdot}MgO{\cdot}2SiO_2$) and gehlenite ($2CaO{\cdot}Al_2O_3{\cdot}SiO_2$) [40, 41]. However, to effectively utilize BF slags for cementitious properties, a high fraction of amorphous phase, must be guaranteed in the slags, which can be dependent on the different cooling process. Figure 4a shows the schematic diagram of typical time–temperature–transformation (TTT) and continuous-cooling-transformation (CCT) curves, where different cooling conditions can result in different microstructures of slag [40]. The slag with cooling path 1 will all form the amorphous phase and the cooling path 2 is the critical cooling rate, where primary crystals form when the cooling rate is less than the critical cooling rate. The slag with cooling paths 3 and 4 through CCT or TTT curves will form crystalline phases with different crystal types and morphologies. According to the utilization purpose of the slag, the structure of the slags can be controlled through selecting an appropriate cooling path, which results in a characteristic physical and chemical property of the slag.

Lin et al. [42] employed a SHTT to detect the isothermal crystallization behavior of typical BF slags. It was found that the growth rate of the crystal first increased and then decreased with the decreasing isothermal temperatures. A critical cooling rate of approximately 540 K/min could be estimated from the TTT diagrams, which indicated that the amorphous phase can be obtained for cooling rates higher than the critical cooling rate. Similar work was also carried out by Qin et al. [43] to study the effects of MgO, Al_2O_3, and basicity (mass ratio of CaO to SiO_2) on the critical cooling rate. Higher MgO content and basicity can increase the critical cooling rate, whereas the critical cooling rate

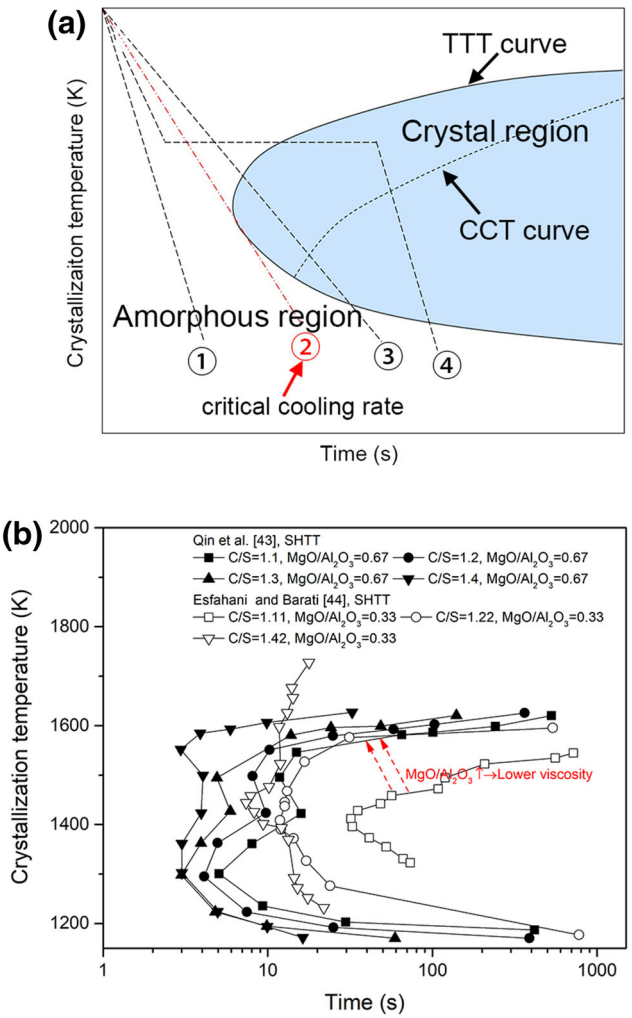

Fig. 4 **a** Schematic diagram of TTT curve and CCT curve, **b** TTT diagrams obtained from SHTT images (Color figure online). Adapted from Kashiwaya et al. [40], Qin et al. [43], and Esfahani and Barati [44]

decreased with the increasing Al_2O_3 content. Esfahani and Barati [44] also found that the higher basicities result in shorter nucleation times and higher crystallization temperatures, which trend was similar to that observed by Qin et al. [43]. From the comparison of the TTT results shown in Fig. 4b, an extended crystal nucleation time was observed for slags at lower MgO/Al_2O_3 ratios for similar basicities, which was caused by the higher viscosity inhibiting mass transfer and therefore delaying crystallization and growth [45]. In addition, for slags with NBO/T $\geq$ 1.6 ($NBO/T = (2x_{CaO} - 2x_{Al_2O_3} + 2x_{MgO}) \div (x_{SiO_2} + 2x_{Al_2O_3})$, non-bridging oxygen atoms over tetrahedrally coordinated atoms) [46], Esfahani and Barati [44] observed equiaxed crystals at higher isothermal temperatures, but observed planar-to-equiaxed crystal transition with lower isothermal temperatures. For slags with NBO/T $<$ 1.6, nucleation and growth were suppressed.

Gan et al. [41] evaluated the crystallization kinetics of molten BF slags under continuous cooling conditions based on DSC measurements. According to the Johnson–Mehl–Avrami–Kolmogorov (JMAK) equation, the crystallization mechanism was controlled by both surface nucleation and one-dimensional growth of rod-like bulk nucleation. Ding et al. [47] applied the directional solidification technology to study the variations in the internal temperatures of the cooled BF slags to estimate the local heat-transfer coefficient and average cooling rate. The average cooling rate gradually decreased from the cooling side to the adiabatic side due to the greater heat resistance and latent heat released, which results in a lower fraction of the amorphous phase in BF slags. Based on their data, a relationship between the average cooling rate of the BF slag and the distribution fraction of amorphous phase along the vertical direction parallel to the heat-removal direction could be established. Considering the importance of amorphous phase relative to cement activity that can be defined as the hydraulic activity of the slag used in the cement, Pal et al. [14] conducted the research and showed that the quenching rate affecting the amorphous phase proportion was the main factor affecting the strength of the slag-containing cement. Although the slag with an amorphous phase proportion as low as 30–65 pct can still be applied, it can show satisfactory performance when the amorphous phase proportion exceeded 90 pct.

Recovery of Valuable Elements from Steelmaking Slags

Unlike the ironmaking slags, there has been comparatively lower utilization of steelmaking slags due to its high content of transition metal oxides including FeO and MnO and high slag basicity with free-CaO. Thus, understanding the behavior of the transition metal oxides is critical to the subsequent recovery, separation, and possible control of the crystallization during cooling of the slag at various cooling rates and atmospheric conditions.

Semykina et al. [48] conducted the kinetic study of divalent iron oxidation in the $CaO–SiO_2–FeO$ slags employing CLSM, where crystal growth and agglomeration of calcium-silicate phases with lengths between 20 and 40 μm could be observed between 1570 K and 1600 K (1297 °C and 1327 °C) [49]. Hematite (Fe_2O_3) with a cubic shape appeared to precipitate at lower temperatures, which would be beneficial to the recovery of Fe through magnetic separation. The separation efficiency can be further enhanced by controlling the oxygen partial pressure to form magnetite (Fe_3O_4) to ensure greater magnetic separation. To consider the implications of MnO in the slag, Semykina et al. [50] also investigated the $CaO–SiO_2–FeO–MnO$ slag system. The TTT diagrams showed greater

crystallization tendency with higher basicity, which is likely due to the enhancement in activity of FeO and MnO in the slag, facilitating the precipitation of FeO_x- and MnO_x-based phases. The combination of CLSM, SEM, and XRD results showed that the spinel containing manganese ferrite can be formed and surrounded by a calcium-silicate phase, but limited information on the kinetics and the substitution of the Mn and Fe into the spinel phase was not described. Similar approaches were also attempted by Li et al. [51, 52] to control the crystallization behavior and subsequent recoveries of Fe and Mn metals as magnetite or manganese ferrite.

Jung and Sohn [53] studied the crystallization of Fe_tO-rich EAF slags employing a combination of CLSM and DTA. Their results showed spinel ($MgAlFeO_4$) to initially precipitate followed by secondary phases of the akermanite ($Ca_2MgSi_2O_7$), merwinite ($Ca_3MgSi_2O_8$), and augite ($CaAlSi_2O_6$) phases. A magnetic Fe-enriched $MgAlFeO_4$ phase and nonmagnetic Fe-depleted amorphous phase could be formed under a controlled cooling rate, as shown in Fig. 5a, which would allow the separation of the Fe-enriched $MgAlFeO_4$ phase and Fe-depleted phase. As a follow-up to their work on localized selective concentration of metal cations within a spinel primary crystal phase, Jung et al. [54] studied the fundamental characteristics of phase separation between an Fe-enriched phase and an amorphous phase highlighting the mechanical dissimilarity between disparate phases. Beyond the control of crystallization, the Fe-depleted amorphous phase with a lower fracture toughness resulted in a finer powder distribution after pulverization. Thus, based on the characteristic particle size distribution between crystalline and amorphous phases after mechanical milling, a magnetic separation between an Fe-enriched crystalline spinel from a Fe-depleted amorphous phase could be improved. In the work of Kim et al. [55], the reduction behavior of FeO in EAF slags with various reductants was studied, and the effects of varying compositions of the reduced EAF slags on the crystallization and elemental distribution were observed and characterized using the CLSM and SEM–EDS. With the reduced EAF slags, the resulting amorphous phase was used as additives in cement with comparable properties to those of the widely used commercial ground-granulated blast furnace slag, as shown in Fig. 5b.

Blanpain and co-workers [56–59] have focused on investigating the metal recovery and slag valorization of steelmaking slags. With suitable additions of C, Al_2O_3, and SiO_2 contents to FeO-containing BOF slags under rapid cooling conditions, metallic Fe could be produced and extracted as a high-grade metal with simultaneous formation of C_2S, C_3S, and an amorphous phase, which could be potentially used as an additive for cement substitutes for construction applications. During the carbothermic

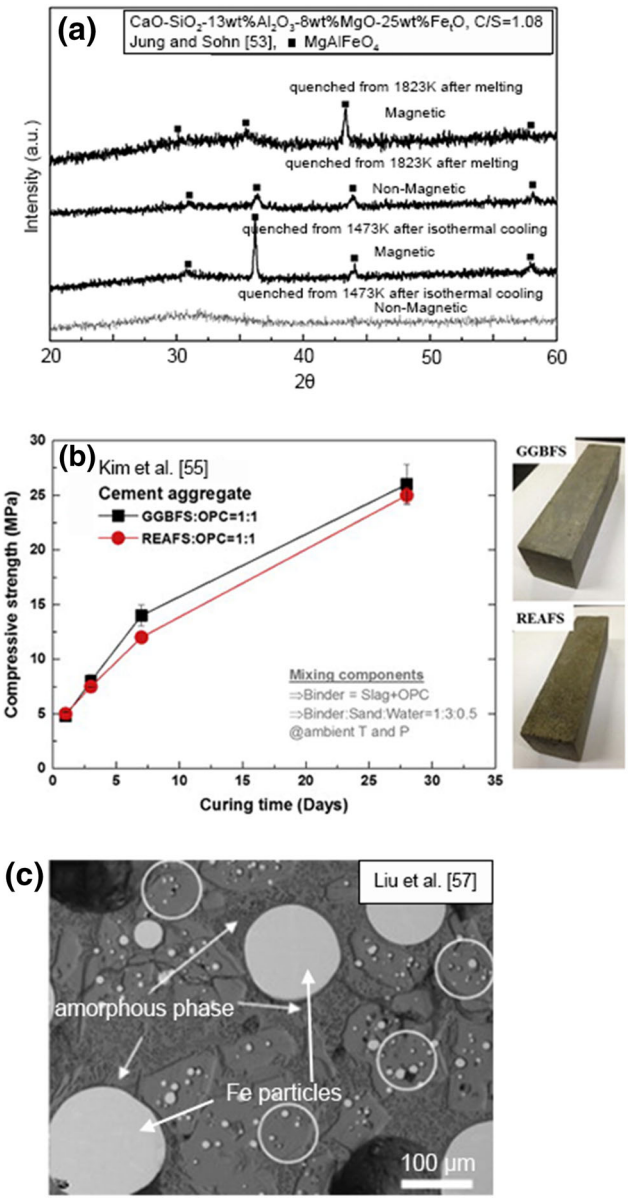

Fig. 5 **a** XRD patterns of the magnetic and nonmagnetic parts of solid slag under different cooling conditions, **b** Compressive strength comparison of standard prismatic specimens produced from supplementary cementitious materials of ground-granulated blast furnace slags (GGFBS) and reduced electric arc furnace slags (REAFS) at ambient temperature and pressure, and **c** After carbothermic reduction, the morphology of metallic Fe recovered with 10 wt pct Al_2O_3 additions (Color figure online). Adapted from Jung and Sohn [53], Kim et al. [55], and Liu et al. [57]

reduction process, both Fe and P could be reduced and concentrated into a spherical metallic phase, where the P was an impurity in the Fe metallic phase. Steelmaking slags can contain on average approximately 3 wt pct of P_2O_5. At specified C additions, a high-grade metallic phase with 98 wt pct Fe could be realized. Furthermore, it was found that a gradual increase in the Al_2O_3 content from 0 to

10 wt pct resulted in larger growth size of the metallic Fe phase from almost lower than 10 μm to higher than 100 μm, as shown in Fig. 5c.

With significant P being present in steelmaking slags and due to its strategic importance in the fields of agriculture and chemical industry, the reclamation of P is essential to ensure the total supply of P from the natural phosphate ore and recycling meets the needs of the various industries [60]. Thus, understanding the mechanism of P distribution in slags and subsequent solidification behavior of P-containing slags is paramount to its effective retrieval and subsequent P recycling. De-phosphorization in steelmaking was actively studied between 1960s and 1980s, which focused on the $CaO–SiO_2–Fe_tO–P_2O_5$ slag system, where the $n Ca_2SiO_4–Ca_3(PO_4)_2$ ($nC_2S–C_3P$) phase was found to be the dominant crystal phase during phosphorous removal [61–64]. Under this premise, numerous studies have focused on the promotion of phosphorus in the $nC_2S–C_3P$ solid-solution phase [65–73]. Wang et al. [16, 74, 75] used DSC to study the crystallization behavior of P-bearing steelmaking slags and correlated to the slag viscosity and structure, where P- and Fe-enriched phases were precipitated. With higher TiO_2 and Al_2O_3 content, C_2S could be reduced from the nC_2S-C_3P phase corresponding to a relative increase in the percentage of phosphorus in the solid solution. When CaF_2 was present, the P-enriched phase transformed to the $Ca_5(PO_4)_3F$, which could not be dissolved in a citric acid solution resulting in low value for utilization as a phosphate fertilizer [69, 72]. Considering that the fertilizer efficiency is determined by the P_2O_5 content and its solubility in citric acid [72], the formation of the $Ca_5(PO_4)_3F$ is detrimental and subsequently the addition of CaF_2 should be minimized in terms of the re-utilization potential. Xie and Wang [76, 77] also investigated the isothermal crystallization behavior of the nC_2S-C_3P solid solutions by using SHTT, where a dendritic nC_2S-C_3P crystal was observed with secondary dendritic arms growing for prolonged holding times during isothermal cooling. Furthermore, the crystallization tendency of nC_2S-C_3P could be improved with higher P_2O_5 content and lower isothermal cooling temperatures, in contrast to Fe_tO additions.

The retrieval of valuable elements such as vanadium from steelmaking slags has also been studied for those integrated steelmakers using vanadium-bearing titaniferous magnetite ores in the ironmaking process [78]. Dong and co-workers [79–84] focused on the enrichment of V in steelmaking slags, where the mechanism of vanadium enrichment was comparable to P existing as $n Ca_2SiO_4–Ca_3(VO_4)_2$ or $n Ca_2SiO_4–Ca_3((V,P)O_4)_2$. Similar to P, higher contents of TiO_2 and Al_2O_3 could enhance the concentration of vanadium in the solid-solution phase. In addition, abundant amounts of alloy elements are generated during the stainless steel production, such as Cr, Ni, Mn, V, Ti, and Mo, which need pretreatment before its application and landfilling, fetching the economic benefits and retarding the environmental pollution [85, 86]. Through the leaching process for the stainless steel slags, the contents of the alloy elements in the slags can meet the standard level, while further disposal of waste water needs to be taken into consideration. It is also reported that Cr and Ni can be separated by magnetic and gravitational methods in some commercial processes [85]. However, the limited utilization seems that more efforts are needed to be made for recovering Cr and Ni through this method.

Due to the refining role of steelmaking slags, a high content of CaO is typically present and free-CaO is often generated in steelmaking slags from the decomposition of Ca_3SiO_5 into Ca_2SiO_4 at about 1573 K (1300 °C) under natural cooling conditions [87]. The presence of free-CaO or MgO and its subsequent expansion through reactions and carbonation limits the use of steelmaking slags in construction materials. Thus, fundamental work on reducing the free-CaO or MgO contained in the steelmaking slags have been conducted. Generally, the free-CaO in steelmaking slags can be minimized by adding SiO_2 or SiO_2-bearing fly ash or gangue, where SiO_2 could react with free-CaO to form a stable calcium-silicate phase [87, 88]. In addition, SiO_2 can react with the CaO present within the calcium-ferrite phase to form Ca_3SiO_5, which can further be transformed to the Ca_2SiO_4 with more additions of SiO_2. The reduced amount of the calcium-ferrite phase has been known to improve the grindability of steelmaking slags. Yin et al. [89] investigated the stabilization of free-CaO by mixing BF slag and BOF industrial slags with basicity values of 1.29 and 3.35, respectively. By mixing the BOF and BF slags at 1723 K (1450 °C) with a mass ratio of 1:4, the free-CaO content decreased from 6.94 wt pct to 0.85 wt pct, as shown in Fig. 6a, b. Carbonization can also be an effective method to eliminate free-CaO in steelmaking slags by forming $CaCO_3$. Peng et al. [88] suggested carbonation of free-CaO can be achieved under CO_2 atmosphere at low oxidized states of the Fe-containing phase, reducing the free-CaO to less than 1 wt pct. Gautier et al. [90] investigated the effect of cooling conditions on the solidified microstructures of BOF slags under oxidizing conditions. Slowly cooled slags resulted in less free-CaO content than rapidly cooled slag, which was attributed to the time allowed for free-CaO to react with iron oxides producing the calcium-ferrite phase. Liu et al. [91] examined the effect of Ar and air on the free-CaO behavior at slow cooling rates and found the free-CaO could be efficiently eliminated under air by oxidizing wustite [RO (FeO–MgO–MnO)] to hematite (Fe_2O_3) and forming brownmillerite ($Ca_2(Al,Fe)_2O_5$), as shown in Fig. 6c, d.

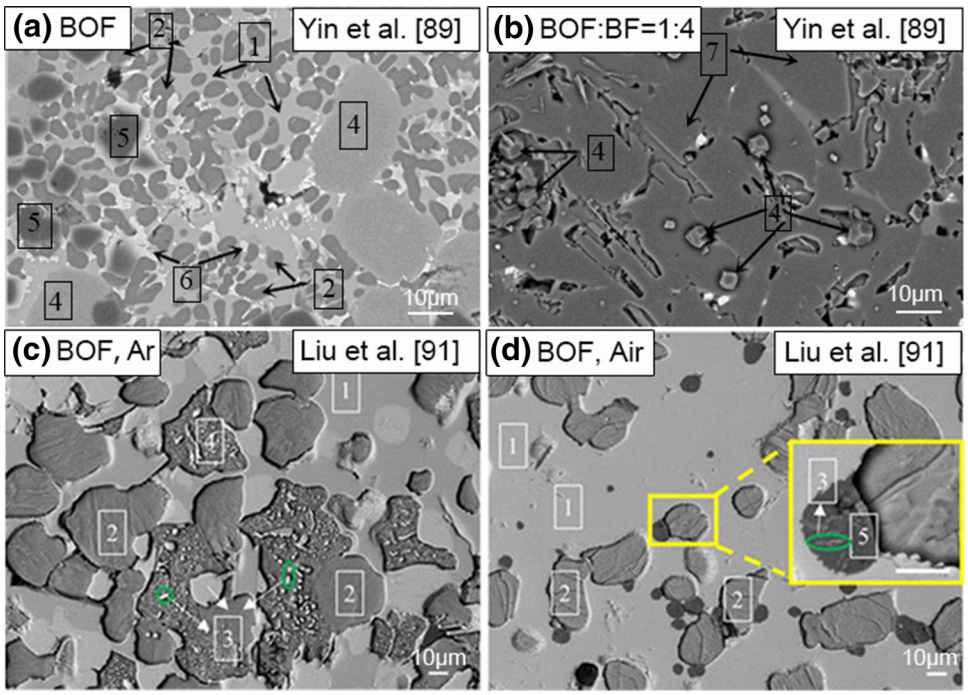

1. $Ca_2(Al,Fe)_2O_5$, 2. Ca_2SiO_4, 3. RO (FeO-MgO-MnO), 4. Free-CaO, 5. MgO, 6. $Ca_2Fe_2O_5$, 7. $Ca_4MgAl_2Si_3O_{14}$

Fig. 6 **a** Microstructures of original BOF slag, **b** microstructures of slags melted at 1723 K (1450 °C) with BOF:BF = 1:4 (mass ratio), **c** microstructures of the BOF slag under Ar atmosphere, and **d** microstructures of the BOF slag under Air atmosphere (Color figure online). Adapted from Yin et al. [89] and Liu et al. [91]

Elemental Separation and Valuable Metal Recovery

Based on the above selective enrichment of the valuable elements in ironmaking and steelmaking slags, some separation efforts have been carried out by some research groups. Guo and co-workers [92–97] investigated the separation of Ti-enriched phase ($CaTiO_3$) from BF slags and P- and Fe-enriched phase ($n Ca_2SiO_4$–$Ca_3(PO_4)_2$ and $MgFe_2O_4$) from steelmaking slags by using gravity-separation method based on the characteristic density of these phases. For Ti-bearing BF slags with the gravity coefficient G of 600, time of 5 min, and temperature of 1563 K (1290 °C), the mass fraction of TiO_2 could reach 52.94 wt pct in the concentrate, while that of the tailing was just 5.88 wt pct, where the recovery ratio of Ti in the concentrate was up to 81.28 wt pct by centrifugal separation. For P-bearing steelmaking slags, the concentrates can be divided into P-enriched phase and Fe-enriched phase, which correlates well with the work of Wang et al. [74], as shown in Fig. 7a. The results shown in Fig. 7b–e were experimental samples subjected to centrifugal force, where the P-enriched phase could be effectively separated from the Fe-enriched phase in steelmaking slags. The uniform P-bearing phase can be intercepted by the bottom filter screen to improve the separation efficiency, where the recovery ratio of P_2O_5 in the P-enriched slag was up to 76.67 wt pct, and that of FeO in the Fe-enriched slag was up to 85.02wt pct. Bao et al. [65–69] employed the magnetic separation method to process the P-enriched phase and Fe-enriched phase in P-bearing steelmaking slags. After the modification by SiO_2, Al_2O_3 and TiO_2, and then the magnetic separation, the recovery of P in the non-magnetic phase can exceed 80 pct. Considering the lower density of the P_2O_5-enriched phase compared to that of the FeO-enriched liquid phase, Miki and Kaneko [98] attempted to use the capillary action to facilitate penetration of an FeO-enriched liquid phase within a sintered CaO crucible to enhance separation. By reheating the slag in a CaO-sintered crucible, 73 wt pct of P_2O_5 was absorbed into the Ca_2SiO_4 phase and 92 wt pct of FeO was absorbed into the remaining liquid slag, where the FeO-enriched liquid phase could be used as an Fe source and the P_2O_5-enriched $2Ca_2SiO_4$ phase could be utilized as a P source. Kitamura and co-workers [99–105] selectively leached phosphorus from steelmaking slags and attempted to use the recovered phosphorus for agriculture purposes. Additions of Na_2SiO_3 or Na_2O promoted the transformation of the P-enriched phase from a $n Ca_2SiO_4$–$Ca_3(PO_4)_2$ to $n Ca_2SiO_4$–Ca_2Na_2-P_2O_9 resulting in higher P solubility. Similar effects were observed for K_2O additions. When the pH of the leachant was controlled between 6 and 5, the furnace-cooled slags showed a considerably higher dissolution rate of P than Fe,

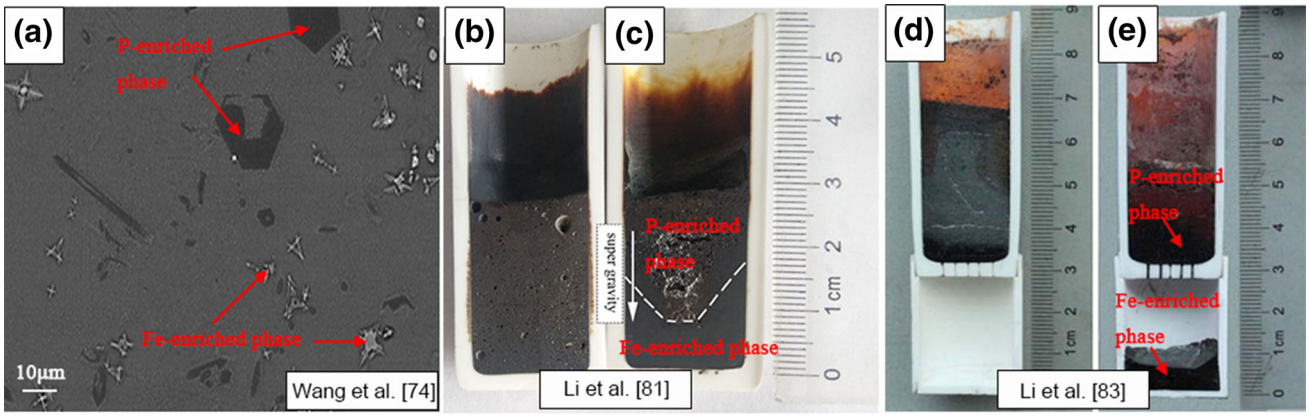

Fig. 7 **a** SEM result of the P-enriched phase and Fe-enriched phase, **b–e** vertical profile of the sample after centrifugal separation compared with the parallel sample: **b** $G = 1$, $T = 1663$ K, $t = 40$ min, **c** $G = 800$, $T = 1663$ K, $t = 40$ min, **d** $G = 1$, $T = 1623$ K, $t = 20$ min, **e** $G = 750$, $T = 1623$ K, $t = 20$ min (Color figure online). Adapted from Wang et al. [74] and Li et al. [81, 83]

resulting in the residue to be high in Fe_2O_3 and low in P_2O_5.

Major Application of Ironmaking and Steelmaking Slags

Internal Reuse of Slags Within the Metallurgical Process

Due to the high CaO content in steelmaking slags, the slag can be used as a fluxing agent in the ironmaking process, which can partially replace commercial limestone and reduce costs. When the content of CaO in the steelmaking slags exceeds 50 wt pct, the steelmaking slags can be used as a sinter flux, partially replacing lime [106]. After optimal quantity steelmaking slag is added to the sinter, the quality of the sinter, the drum index, and the sintering rate can be improved facilitating sintering ball formation and speed. The steelmaking slags can also be used as iron smelting agents to recover iron from steelmaking slags. Injection of slag formers through the tuyeres, such as BOF slag, can lower the melting point of the fuel ash and better form liquid slags for stable BF operations [107]. However, the simple recirculation of the steelmaking slags in the metallurgical process will inevitably result in P accumulation, which will likely aggravate downstream de-phosphorization. Thus, the amount of spent metallurgical refining slags recycled within the metallurgical process could be limited [7].

Civil Construction Application of Slags

Typical Ti-free BF slag can generally substitute up to 40–50 wt pct of Portland cement [108], and this limit is mainly due to the lower early strength and delayed setting time. The reactivity of the mixed cement with Ti-free BF slags can be improved through fine grinding and improved mechanical activation [109]. With higher specific surface area, the reactivity is enhanced improving the strength and solidification properties of the cement or concrete [110]. Kumar et al. [108, 111] investigated the mechanical activation of granulated BF slag and its effect on the properties and structure of the Portland slag cement. It was found that after 28 days, the mechanical strength of the Portland cement substituted with 85 wt pct BF slags with a median size of 10 μm was comparable to that of a commercial cement containing 40 wt pct BF slag with a median size about 90 μm.

On the other hand, due to the high content of TiO_2 in the Ti-bearing BF slags, it has a strong ability to crystallize making it difficult to produce an amorphous phase during natural cooling or water quenching that result in poor activity of the cement during setting. Although Ti-bearing BF slags can be used for bricks or other construction materials that satisfy quality indicators [112], this results in greater waste of titanium resources in terms of today's sustainable development concept. The current lower utilization rate of Ti-bearing BF slags has forced us to develop other approaches for massive consumption of Ti-bearing BF slags. Jiao et al. [113] studied the use of a liquid iron cathode electrolysis process to prepare Si–Ti alloys from Ti-bearing BF slags, where a low deposition potential of about 2.0 V and relatively high current efficiency of 69.8 pct could be obtained with a residue that can be used for cement applications.

Steelmaking slags can also be used as cement aggregates and road construction materials. Li et al. [114] showed that the properties of the typical clinker-poor steelmaking slag cement with a mixture of steelmaking slags of 40 wt pct, BF slags of 40 wt pct, clinker of 15 wt pct, gypsum of 5 wt pct, and composite alkali activators of 2.5 wt pct were

comparable to those of the standard of grade 42.5 Portland cement. However, steelmaking slags had poor grindability, large particles, and less cementitious minerals. In addition, the activities of C_2S and C_3S in steelmaking slags are much lower than cement clinkers, which make them less favorable for complete substitution of typical Portland cement. Furthermore, β-C_2S, which is the main component in steelmaking slags, has essentially negligible cementitious properties resulting in lower strength of the prepared cement [115]. Although steelmaking slags used in road construction can have increased bearing capacity in roadbed applications, the excessive free-CaO in the steelmaking slags can react with water resulting in volume expansion and poor stability. Thus, the utilization of steelmaking slags as a stand-alone product in civil construction application is highly unlikely unless preprocessing can be archived prior to cooling.

Building Materials Application of Slags

Ti-free BF slags and steelmaking slags can also be used to produce mineral wool for insulation. Zhao et al. [13, 116] investigated the preparation of mineral wool using Ti-free BF slag modified by fly ash. By controlling the BF slag between 60 and 80 wt pct, its viscosity and crystallization temperature could be optimally controlled to produce mineral wool. The morphology of slag fibers is shown in Fig. 8a and has been expanded to actual industrial applications, as shown in Fig. 8b, c. Compared with traditional methods, the direct production of mineral wool with molten slags from process byproducts can save an equivalent of 346.3 kg coal for each ton of slag wool reducing the pollutant emission by 90 pct. Alves et al. [117] also attempted to use steelmaking slag and residues from granite cuttings as the raw materials into the production of rock wool. The results indicated that the major criteria for rock wool produced through process byproducts market requirements in thermal insulation and fire-protection characteristics.

Future Potential Treatment of Slags

Although there exist many similar attempts of consuming smaller quantities of metallurgical slags, balancing the evolution of enormous metallurgical slags and its utilization should be considered in terms of two perspectives for the future. One perspective is to fundamentally reduce the amount of slag produced during processing [118, 119]. Slags have been studied and designed to improve the refining capacity for higher quality and to optimize its thermophysical properties for a wide range of process applications. However, in the light of excessive formation of metallurgical slags and utilization capacity limits, a new approach to the original concept of slags or processing is needed to reduce the total slag output in terms of the overall ironmaking and steelmaking process, while maintaining sufficient refining capacity. Brämming and Wikström [120] found that injecting highly basic BOF slags containing CaO through the blast furnace tuyere can reduce the total amount of slag output, which also has an advantage of reusing BOF slags and further reducing the melting point of the fuel ash in the PCI (pulverized coal injection) practice. By lowering the overall slag volume produced, metal productivity increases, and the energy efficiency is likely increased. The other perspective is to find novel uses for slags in other industries beyond commonly attempted ones for slags. In the work of Piatak [121], legacy steelmaking slags in the Chicago area of the United States had potential to treat phosphate-rich or acidic waters, but suggested that the pH and trace-element contents of the resulting solutions could require further examination. Chou et al. [122] conducted long-term monitoring of the demersal fish community in the steelmaking slag disposal area along the coast in Taiwan, where a reef-like habitat was constructed in the steelmaking slag-dumped seawater with a higher diversity of fish than the original sandy bottom. Similar work was attempted by Miyata et al. [123], where granular steelmaking slags were placed on the seabed 20 m

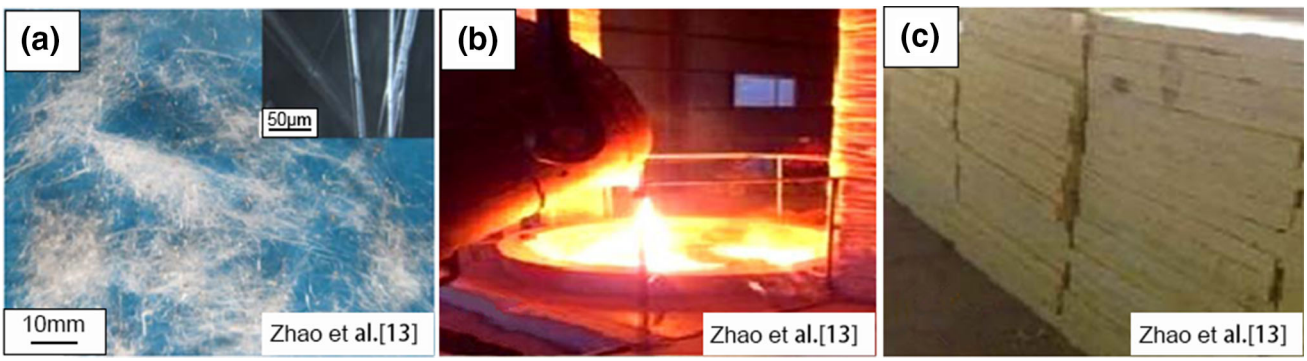

Fig. 8 **a** Morphology of slag fibers produced at 1723 K (1450 °C), **b** molten slag pouring from the tank into the modified furnace, and **c** mineral wool insulation board product (Color figure online). Reproduced with permission from Zhao et al. [13]

in depth and compared with a reference granite sample of similar conditions. It was found that steelmaking slags were more effective in inhibiting sulfides damaging living organisms and promoted adhesion and multiplication of phytoplankton. These novel potential uses require further study, but investigations to expand the scope of the application of metallurgical slags in both internal reuse and other external industries are necessary to ensure a sustainable steel industry.

Conclusions

This work reviewed both the fundamental aspects of slag recycling and current major applications. Understanding the fundamental crystallization behavior and thermodynamics of phase evolution during cooling and the kinetics of phase transformation allows for enhanced control of the evolved phases and elemental redistribution in the as-cooled slags. Internal reutilization of slags and applications in the construction and building materials have also been addressed. Future applications for steelmaking slags have also been reviewed to enhance the sustainability potential of metallurgical slags in the long term.

Acknowledgements This work was supported by the Brain Korea 21 Plus Project and Basic Science Research Program through the National Research Foundation of Korea (NRF) funded by the Ministry of Science, ICT & Future Planning (2018R1A2B2006609).

Compliance with Ethical Standards

Conflict of interest On behalf of all authors, the corresponding author declares that there are no conflicts of interest.

References

1. Worldsteel Association: https://www.worldsteel.org/en/dam/jcr:3e275c73-6f11-4e7f-a5d8-23d9bc5c508f/Steel%2520Statistical%520Yearbook%25202017_updated%2520version090518.pdf
2. Guo J, Bao Y, Wang M (2018) Steel slag in China: treatment, recycling, and management. Waste Manage (Oxford) 78:318–330
3. Nippon Slag Association. http://www.slg.jp/e/slag/kind.html
4. Matino I, Colla V, Romaniello L, Rosito F, Portulano L (2015) Simulation techniques for an efficient use of resources: an overview for the steelmaking field. In: 2015 World Congress Sustainable Technologies (WCST), IEEE, pp 48–54
5. Yellishetty M, Mudd GM (2014) Substance flow analysis of steel and long term sustainability of iron ore resources in Australia, Brazil, China and India. J Clean Prod 84:400–410
6. Vaverka J, Sakurai K (2014) Quantitative determination of free lime amount in steelmaking slag by X-ray diffraction. ISIJ Int 54:1334–1337
7. Wang ZJ, Shu QF, Seetharaman S, Zhang M, Guo M, Zhang ZT (2015) Effect of P_2O_5 and Fe_tO on the viscosity and slag structure in steelmaking slags. Metall Mater Trans B 12:758–765
8. Gomes JF, Ascenço CG (2006) Leaching of heavy metals from steelmaking slags. Rev Metal Madrid 42:409–416
9. Wang X, Mao Y, Liu X, Zhu Y (1990) Study on crystallization behavior for blast furnace slag containing TiO_2. J Iron Steel Res 3:1–6
10. Wang X, Mao Y, Xie D, Zhu Y (1993) Crystallization behavior of the blast furnace slag with titanium at the reduction state. J Anhui Univ of Technol 19–23
11. Wang MH, Du HX, Sui ZT (2000) Recovery of titanium from rich titanium blast furnace slag by sulfate method. Multi Utility Miner Res 4:5–8
12. Wang M, Li L, Li Z, Zhang L, Tu G, Sui Z (2006) Effect of oxidization on enrichment behavior of TiO_2 in titanium-bearing slag. Rare Met 25:106–110
13. Zhao D, Zhang Z, Tang X, Liu L, Wang X (2014) Preparation of slag wool by integrated waste-heat recovery and resource recycling of molten blast furnace slags: from fundamental to industrial application. Energies 7:3121–3135
14. Pal SC, Mukherjee A, Pathak SR (2003) Investigation of hydraulic activity of ground granulated blast furnace slag in concrete. Cem Concr Res 33:1481–1486
15. Min DJ, Tsukihashi F (2017) Recent advances in understanding physical properties of metallurgical slags. Met Mater Int 23:1–19
16. Wang Z, Sun Y, Seetharaman S, Zhang M, Guo M, Guo Z, Zhang Z (2016) Viscous flow and crystallization behaviors of P-bearing steelmaking slags with varying fluorine content. ISIJ Int 56:546–553
17. Das B, Prakash S, Reddy P, Misra V (2007) An overview of utilization of slag and sludge from steel industries. Resour Conserv Recycl 50:40–57
18. Escalante JI, Gómez LY, Johal KK, Mendoza G, Mancha H, Méndez J (2001) Reactivity of blast-furnace slag in Portland cement blends hydrated under different conditions. Cement Concrete Res 31:1403–1409
19. Itoh T (2004) Rapid discrimination of the character of the water-cooled blast furnace slag used for Portland slag cement. J Mater Sci 39:2191–2193
20. Gong XJ, Jia F, Liu R, Ye F, Guan H, Wang R, Guo G (2014) Study on preparation and photocatalytic activity of photocatalyst made from Ti-bearing blast furnace slag. Appl Mech Mater 526:33–39
21. Lei X, Xue X, He Y (2012) Preparation of UV-visible light responsive photocatalyst from titania-bearing blast furnace slag modified with $(NH_4)_2SO_4$. Trans Nonferrous Met Soc 22:1771–1777
22. Li Z, Xu C (2007) The smelting process of titanium-silicon ferroalloy using blast furnace titaniferous slag. ISIJ Int 36:279–283
23. Li J, Zhang ZT, Wang XD (2012) Precipitation behavior of Ti enriched phase in Ti bearing slag. Ironmak Steelmak 39:414–418
24. Li J, Wang X, Zhang Z (2011) Crystallization behavior of rutile in the synthesized Ti-bearing blast furnace slag using single hot thermocouple technique. ISIJ Int 51:1396–1402
25. Li J, Zhang Z, Zhang M, Guo M, Wang X (2011) The influence of SiO2 on the extraction of Ti element from Ti-bearing blast furnace slag. Steel Res Int 82:607–614
26. Li J, Zhang Z, Liu L, Wang W, Wang X (2013) Influence of basicity and TiO_2 content on the precipitation behavior of the Ti-bearing blast furnace slags. ISIJ Int 53:1696–1703
27. Hu M, Wei R, Gao L, Liu L, Bai C (2018) Effect of the basicity on the crystallization behavior of titanium bearing blast furnace slag. High Temp Mater Proc 37:193–200

28. Hu M, Qu Z, Lv X, Gan Y (2016) Precipitation behavior of titanium bearing blast furnace slag. In: Proceedings of the 10th international conference on molten slags, fluxes and salts, pp 1261–1270
29. Hu M, Wei R, Yin F, Liu L, Deng Q (2016) Effect of TiO_2 content on the crystallization behavior of titanium-bearing blast furnace slag. JOM 68:2502–2510
30. Liu L, Hu M, Xu Y, Bai C, Gan Y (2015) Structure, growth process, and growth mechanism of perovskite in high-titanium-bearing blast furnace slag. Metall Mater Trans B 46:1751–1759
31. Liu L, Hu M, Bai C, Lv X, Wen L, Zhang S (2014) In situ observation of the crystallization process of perovskite in titanium-bearing blast furnace slag. Min Proc Ext Met 123:241–245
32. Hu M, Liu L, Lv X, Bai C, Zhang S (2014) Crystallization behavior of perovskite in the synthesized high-titanium-bearing blast furnace slag using confocal scanning laser microscope. Metall Mater Trans B 45:76–85
33. Zhang W, Zhang L, Feng NX (2013) Effect of oxidation on phase transformation in Ti-bearing blast furnace slag. Adv Mater Res 641–642:363–366
34. Zhang W, Zhang L, Zhang J, Feng NX (2012) Crystallization and coarsening kinetics of rutile phase in modified Ti-bearing blast furnace slag. Ind Eng Chem Res 51:12294–12298
35. Wang Z, Liu X, Zhang L, Zhu Q (2016) The influence of composition on crystallization and liberation behavior of Ti-rich phase in Ti-bearing slags. Trans Indian Inst Met 69:97–105
36. Li Z, Li J, Sun Y, Seetharaman S, Liu L, Wang X, Zhang Z (2016) Effect of Al_2O_3 addition on the precipitated phase transformation in Ti-bearing blast furnace slags. Metall Mater Trans B 47:1390–1399
37. Sun Y, Li Z, Liu L, Wang X, Zhang Z (2015) Co-modification and crystalline-control of Ti-bearing blast furnace slags. ISIJ Int 55:158–165
38. Li Z, Sun Y, Liu L, Wang X, Zhang Z (2015) Enhancement of rutile formation by ZrO_2 addition in Ti-bearing blast furnace slags. ISIJ Int 55:1384–1389
39. Kim GH, Sohn I (2014) Role of B_2O_3 on the viscosity and structure in the $CaO–Al_2O_3–Na_2O$-based system. Metall Mater Trans B 45:86–95
40. Kashiwaya Y, Nakauchi T, Son PK, Akiyama S, Ishii K (2007) Crystallization behaviors concerned with TTT and CCT diagrams of blast furnace slag using hot thermocouple technique. ISIJ Int 47:44–52
41. Gan L, Zhang C, Zhou J, Shangguan F (2012) Continuous cooling crystallization kinetics of a molten blast furnace slag. J Non-Cryst Solids 358:20–24
42. Lin B, Wang H, Zhu X, Liao Q, Ding B (2016) Crystallization properties of molten blast furnace slag at different cooling rates. Appl Therm Eng 96:432–440
43. Qin Y, Lv X, Zhang J (2016) Effect of composition on the crystallization behavior of blast furnace slag using single hot thermocouple technique. Ironmak Steelmak 44:23–27
44. Esfahani S, Barati M (2016) Effect of slag composition on the crystallization of synthetic $CaO–SiO_2–Al_2O_3–MgO$ slags: part I—crystallization behavior. J Non-Cryst Solids 436:35–43
45. Zhang X, Jiang T, Xue X, Hu B (2016) Influence of MgO/Al_2O_3 ratio on viscosity of blast furnace slag with high Al_2O_3 content. Steel Res Int 87:87–94
46. Kowalski M, Spencer PJ, Neuschuetz D (1995) Slag Atlas, 2nd edn. Verlag Stahleisen GmbH, Dusseldorf
47. Ding B, Wang H, Zhu X, He XY, Liao Q, Tan Y (2016) Crystallization behaviors of blast furnace (BF) slag in a phase-change cooling process. Energ Fuel 30:3331–3339
48. Semykina A, Nakano J, Sridhar S, Shatokha V, Seetharaman S (2010) Confocal microscopic studies on evolution of crystals during oxidation of the $FeO–CaO–SiO_2–MnO$ slags. Metall Mater Trans B 41:940–945
49. Semykina A, Nakano J, Sridhar S, Shatokha V, Seetharaman S (2011) Confocal scanning laser microscopy studies of crystal growth during oxidation of a liquid $FeO–CaO–SiO_2$ slag. Metall Mater Trans B 42:471–476
50. Semykina A, Seetharaman S (2011) Recovery of manganese ferrite in nanoform from the metallurgical slags. Metall Mater Trans B 42:2–4
51. Li J, Bhattacharjee D, Hu X, Zhang D, Sridhar S, Li Z (2017) Development of a novel process for energy and materials recovery in steelmaking slags. Min Proc Ext Met Rev 126:94–105
52. Li J, Bhattacharjee D, Hu X, Zhang D, Sridhar S, Li Z (2017) Crystallization behavior of liquid $CaO–SiO_2–FeO–MnO$ slags in moist gas atmospheres. In: Fifth international slag valorisation symposium, pp 117–120
53. Jung SS, Sohn I (2014) Crystallization control for remediation of an Fe_tO-rich $CaO–SiO_2–Al_2O_3–MgO$ EAF waste slag. Environ Sci Technol 48:1886–1892
54. Jung SS, Jung K, Sohn I (2016) Selective separation of Fe-concentrates in EAF slags using mechanical dissimilarity of solid phases. Metall Mater Trans A 48:1–10
55. Kim HS, Kim KS, Jung SS, Hwang JI, Choi JS, Sohn I (2015) Valorization of electric arc furnace primary steelmaking slags for cement applications. Waste Manage 41:85–93
56. Liu C, Guo M, Pandelaers L, Blanpain B, Huang S, Wollants P (2017) Metal recovery from bof steel slag by carbo-thermic reduction. BHM 162:258–262
57. Liu C, Huang S, Wollants P, Blanpain B, Guo M (2017) Valorization of BOF steel slag by reduction and phase modification: metal recovery and slag valorization. Metall Mater Trans B 48:1602–1612
58. Wang X, Geysen D, Gerven PJ, Blanpain B, Guo M (2017) Characterization of landfilled stainless steel slags in view of metal recovery. Front Chem Sci Eng 11:1–10
59. Fan Y, Zhang L, Volski V, Vandenbosch GAE, Blanpain B, Guo M (2017) Utilization of stainless-steel furnace dust as an admixture for synthesis of cement-based electromagnetic interference shielding composites. Sci Rep 7:15361–15368
60. Matsubae Yokoyama K, Kubo H, Nakajima K, Nagasaka T (2009) A material flow analysis of phosphorus in Japan. J Ind Ecol 13:687–705
61. Kor G (1977) Effect of fluorspar and other fluxes on slag-metal equilibria involving phosphorus and sulfur. Metall Trans B 8:107–113
62. Suito H, Inoue R (1982) Effect of calcium fluoride on phosphorus distribution between MgO saturated slags of the system $CaO–MgO–FeO_x–SiO_2$ and liquid iron. ISIJ Int 22:869–877
63. Berak J, Tomczakh I (1972) Phase equilibria in system $Ca_3(PO_4)_2$-CaF_2. Roczniki Chemii 46:2157–2164
64. Ono H, Inagaki A, Masui T, Narita H, Nosaka S, Mitsuo T, Gohda S (1981) Removal of phosphorus from ID-converter slag by floating separation of dicalcium silicate during solidification. ISIJ Int 21:135–144
65. Lin L, Bao Y, Wang M, Zhou H, Zhang L (2013) Influence of SiO_2 modification on phosphorus enrichment in P bearing steelmaking slag. Ironmak Steelmak 40:521–527
66. Lin L, Bao YP, Wang M, Jiang W, Zhou HM (2014) Separation and recovery of phosphorus from P-bearing steelmaking slag. J Iron Steel Res Int 21:496–502
67. Lin L, Bao YP, Wang M, Jiang W, Zhou HM (2014) P_2O_5 solubility behavior and resource utilization of P-bearing slag. ISIJ Int 54:2746–2753

68. Lin L, Bao YP, Wang M, Zhou HM (2014) Influence of Al_2O_3 modification on phosphorus enrichment in P bearing steelmaking slag. Ironmak Steelmak 41:193–198
69. Lin L, Bao YP, Yang Q, Wang M, Jiang W (2015) Effect of CaF_2 and SiO_2 modification on phosphorus utilization in P-bearing slag. Ironmak Steelmak 42:331–338
70. Wu XR, Wang P, Li LS, Wu ZJ, Chen RH (2013) Distribution and enrichment of phosphorus in solidified BOF steelmaking slag. Ironmak Steelmak 38:185–188
71. Diao J, Ke Z, Jiang L, Zhang T, Xie B (2016) Influence of Al_2O_3 modification on phosphorus enrichment in high phosphorus slag. Min Proc Ext Met Rev 152:103–108
72. Diao J, Xie B, Wang YH, Guo X (2010) Effect of fluorine on the minerals phase and citric acid solubility of $CaO–SiO_2–Fe_tO–P_2O_5–CaF_2$ system. ISIJ Int 50:768–770
73. Diao J, Xie B, Wang YH, Guo X (2012) Recovery of phosphorus from dephosphorization slag produced by duplex high phosphorus hot metal refining. ISIJ Int 52:955–959
74. Wang Z, Sun Y, Seetharaman S, Zhang M, Zhang Z (2017) Investigation on viscosity and nonisothermal crystallization behavior of P-bearing steelmaking slags with varying TiO_2 content. Metall Mater Trans B 48:527–537
75. Wang Z, Sun Y, Seetharaman S, Zhang M, Guo M, Zhang Z (2015) Selective crystallization behavior of $CaO–SiO_2–Al_2O_3–MgO–FetO–P_2O_5$ steelmaking slags modified through P_2O_5 and Al_2O_3. Metall Mater Trans B 46:2246–2254
76. Xie S, Wang W (2016) Isothermal crystallization study of ($2CaO·SiO_2–3CaO·P_2O_5$) solid solution in the 45 mass% CaO–30 mass% SiO_2–20 mass% FeO_{t-5} mass% P_2O_5 system at 1623 K. Steel Res Int 86:1622–1627
77. Xie S, Wang W (2016) Crystallization kinetics study of the ($2CaO·SiO_2$-$3CaO·P_2O_5$) solid solution in the multiphase dephosphorization flux. Steel Res Int 87:376–385
78. Samanta S, Goswami MC, Baidya TK, Mukherjee S, Dey R (2013) Mineralogy and carbothermal reduction behavior of vanadium-bearing titaniferous magnetite ore in Eastern India. Int J Min Met Mater 20:917–924
79. Li LS, Wu XR, Yu L, Dong YC (2008) Effect of TiO_2 on crystallization of V concentrating phase in V bearing steelmaking slag. Ironmak Steelmak 35:367–370
80. Wu X, Li L, Dong Y (2011) Enrichment and crystallization of vanadium in factory steel slag. Metallurgist 55:401–409
81. Dong Y, Wu X, Li L (2005) Precipitation and growth of V-concentrating phase in synthetic V-bearing steelmaking slag. ISIJ Int 45:1238–1242
82. Li L, Wu L, Su Y, Yu L, Wu X, Dong Y (2008) Influence of Al_2O_3 on vanadium concentration in V-bearing steelmaking slag. Acta Metall Sin 44:603–608
83. Wu X, Li L, Dong Y (2007) Influence of P_2O_5 on crystallization of V-concentrating phase in V-bearing steelmaking slag. Ironmak Steelmak 35:367–370
84. Wu XR (2005) Experimental crystallization of synthetic V-bearing steelmaking slag with Al_2O_3 doped. J Wuhan Univ Technol 20:63–66
85. Shen H, Forssberg E (2003) An overview of recovery of metals from slags. Waste Manag 23:933–949
86. Lopez FA, Lopez-Delgado A, Belcazar N (1997) Physicochemical and mechanical properties of EAF and AOD slags. Associazione Italiana di Metallurgia (Italy) 53:417–426
87. Zhou Y, Fang S, Dong Y, Liu H (2010) Role of SiO_2 in the steel slags by modifying. J Chin Rare Earth Soc 28:537–540
88. Peng B, Yue C, Huang S, Zhang M, Guo M, Hu T (2015) CO_2 modification and thermodynamic property of hot steel slag. Environ Eng 33:100–102
89. Yin X, Zhang C, Wang G, Yang J, Cai Y, Zhao C (2018) Free CaO stabilization by mixing of BF slag and BOF slag in molten state. Ironmak Steelmak 6:1–9
90. Gautier M, Poirier J, Bodénan F, Franceschini G, Veron E (2013) Basic oxygen furnace (BOF) slag cooling: laboratory characteristics and prediction calculations. Int J Miner Process 123:94–101
91. Liu C, Guo M, Pandelaers L, Blanpain B, Huang S (2016) Stabilization of free lime in BOF slag by melting and solidification in air. Metall Mater Trans B 47:1–4
92. Gao J, Zhong Y, Guo L, Guo Z (2016) Separation of iron phase and P-bearing slag phase from gaseous-reduced, high-phosphorous oolitic iron ore at 1473 K (1200 & #xB0;C) by super gravity. Metall Mater Trans B 47:1080–1092
93. Gao JT, Guo L, Zhong YW, Ren HR, Guo ZC (2016) Removal of phosphorus-rich phase from high-phosphorous iron ore by melt separation at 1573 K in a super-gravity field. Int J Min Met Mater 23:743–750
94. Li C, Gao J, Guo Z (2016) Isothermal enrichment of P-concentrating phase from $CaO–SiO_2–FeO–MgO–P_2O_5$ melt with super gravity. ISIJ Int 56:759–764
95. Li C, Gao J, Guo Z (2016) Separation of phosphorus- and iron-enriched phase from $CaO–SiO_2–FeO–MgO–P_2O_5$ melt with super gravity. Metall Mater Trans B 47:1516–1519
96. Li C, Gao J, Wang Z, Ren H, Guo Z (2017) Separation of Fe-bearing and P-bearing phase from the steelmaking slag by super gravity. ISIJ Int 57:767–769
97. Li C, Gao JT, Wang FQ, Guo ZC (2016) Enriching Fe-bearing and P-bearing phases from steelmaking slag melt by super gravity. Ironmak Steelmak 45:44–49
98. Miki T, Kaneko S (2015) Separation of FeO and P_2O_5 from steelmaking slag utilizing capillary action. ISIJ Int 55:142–148
99. Du CM, Gao X, Kim SJ, Ueda S, Kitamura SY (2016) Effects of acid and Na_2SiO_3 modification on the dissolution behavior of $2CaO·SiO_2–3CaO·P_2O_5$ solid solution in aqueous solutions. ISIJ Int 56:1436–1444
100. Du CM, Gao X, Ueda S, Kitamura SY (2017) Effect of Na_2O addition on phosphorus dissolution from steelmaking slag with high P_2O_5 content. J Sustain Metall 3:1–12
101. Du CM, Gao X, Ueda S, Kitamura SY (2017) Effects of cooling rate and acid on extracting soluble phosphorus from slag with high P_2O_5 content by selective leaching. ISIJ Int 57:487–496
102. Du C, Gao X, Ueda S, Kitamura S (2018) Recovery of phosphorus from modified steelmaking slag with high P_2O_5 content via leaching and precipitation. ISIJ Int 58:833–841
103. Du CM, Gao X, Ueda S, Kitamura SY (2018) Distribution of P_2O_5 and Na_2O between solid solution and liquid phase in the $CaO–SiO_2–Fe_2O_3–P_2O_5–Na_2O$ slag system with high P_2O_5 content. Metall Mater Trans B 49:181–189
104. Du C, Gao X, Ueda S, Kitamura S (2018) Optimum conditions for phosphorus recovery from steelmaking slag with high P_2O_5 content by selective leaching. ISIJ Int 58:860–868
105. Numata M, Maruoka N, Kim SJ, Kitamura SY (2014) Fundamental experiment to extract phosphorous selectively from steelmaking slag by leaching. ISIJ Int 54:1983–1990
106. Deng Q, Wang Q, Huang Q, Wang H (2010) Analysis on the approaches of utilization for steel slag with the analytic hierarchy process. Met Mine 1:170–174
107. Ma J (2016) Injection of flux into the blast furnace via tuyeres for optimizing slag formation. ISIJ Int 39:697–704
108. Kumar S, Bandopadhyay A, Rajinikanth V, Alex TC, Kumar R (2004) Improved processing of blended slag cement through mechanical activation. J Mater Sci 39:3449–3452
109. Barnett SJ, Soutsos MN, Bungey JH, Millard SG (2004) Fast-track concrete construction using cement replacement materials. In: Proceedings of the eighth CANMET/ACI international

conference on fly ash, silica fume, slag, and natural Pozzolans in concrete, ACI SP-221, vol 221. American Concrete Institute, Farmington Hills, pp 135–151
110. Soutsos MN, Barnett SJ, Bungey JH, Millard SG (2005) Fast track construction with high strength concrete mixes containing ground granulated blast furnace slag. In: International symposium on the utilization of high strength/high-performance concrete, vol 228, pp 255–270
111. Kumar S, Kumar R, Bandopadhyay A, Alex TC, Kumar BR, Das SK, Mehrotra SP (2008) Mechanical activation of granulated blast furnace slag and its effect on the properties and structure of portland slag cement. Cem Concr Compos 30:679–685
112. Wang HB, Cheng XL, Sun XY, Qiang CD (2009) Study on preparation of sintering slag brick using blast furnace slag containing titanium. Multipurp Util Miner Resour 1:36–39
113. Jiao H, Tian D, Wang S, Zhu J, Jiao S (2017) Direct preparation of titanium alloys from Ti-bearing blast furnace Slag. J Electrochem Soc 164:511–516
114. Li Z, Zhou ZH, Liu FT, Li Y, Shan LF, Cheng X (2009) Research on the hydrating mechanism of clinker-poor steel slag cement. J Wuhan Univ Technol 31:139–143
115. Yi H, Xu G, Cheng H, Wang J, Wan Y, Chen H (2012) An overview of utilization of steel slag. Procedia Environ Sci 16:791–801
116. Zhao D, Zhang Z, Liu L, Wang X (2015) Investigation on slag fiber characteristics: mechanical property and anti-corrosion performance. Ceram Int 41:5677–5687
117. Alves JO, Espinosa DCR, Tenório JAS (2015) Recovery of steelmaking slag and granite waste in the production of rock wool. J Mater Res 18:204–211
118. Matsuura H, Hu X, Tsukihashi F (2012) Improvement of function and utilization of steelmaking slag. In: Ninth international conference on molten slags, fluxes and salts
119. Dippenaar R (2005) Industrial uses of slag: the use and re-use of iron and steelmaking slags. Ironmak Steelmak 32:35–46
120. Brämming M, Wikström JO (2010) A blast furnace view on slags. Scand J Metall 31:88–99
121. Piatak NM (2018) Environmental characteristics and utilization potential of metallurgical slag. Environ Geochem 100:100. https://doi.org/10.1016/b978-0-444-63763-5.00020-3
122. Chou W, Tew K, Fang L (2002) Long-term monitoring of the demersal fish community in a steel-slag disposal area in the coastal waters of Kaohsiung, Taiwan. ICES J Mar Sci 59:238–242
123. Miyata Y, Sato Y, Shimizu S, Oyamada K (2009) Environment improvement in the sea bottom by steelmaking slag. JFE Technical Report No. 13, pp 41–45